NANO LETTERS

pubs.acs.org/NanoLett

One-Way Traffic of a Viral Motor Channel for Double-Stranded DNA Translocation

Peng Jing,† Farzin Haque,† Dan Shu, Carlo Montemagno, and Peixuan Guo*

Nanobiomedical Center, College of Engineering and College of Medicine, University of Cincinnati, Cincinnati, Ohio 45267

ABSTRACT Linear double-stranded DNA (dsDNA) viruses package their genome into a procapsid using an ATP-driven nanomotor. Here we report that bacteriophage phi29 DNA packaging motor exercises a one-way traffic property for dsDNA translocation from N-terminal entrance to C-terminal exit with a valve mechanism in DNA packaging, as demonstrated by voltage ramping, electrode polarity switching, and sedimentation force assessment. Without the use of gating control as found in other biological channels, the observed single direction dsDNA transportation provides a novel system with a natural valve to control dsDNA loading and gene delivery in bioreactors, liposomes, or high throughput DNA sequencing apparatus.

KEYWORDS Viral assembly, nanotechnology, nanostructure, nanobiotechnology, nanomedicine, bacteriophage phi29, liposomes, ion channel, rectification, DNA packaging, nanomotors, membrane channel

A striking feature in the assembly of many linear double-stranded DNA (dsDNA) viruses is the packaging of their genome within a preformed procapsid. This entropically unfavorable process is accomplished by an ATP-driven motor.[1−6] The novelty and ingenious design of viral DNA packaging motors and their mechanism of action have provoked a broad range of interest among scientists in nanotechnology, biophysics, RNA biochemistry, virology, and therapeutics. In bacterial virus phi29, the motor is composed of a protein enzyme gp16, serving as a part of the ATPase, and six pRNAs (packaging RNA[7]) that form a ring to gear the motor[7−9] using one ATP to package 2[2] or 2.5[10] base pairs of DNA. The protein hub of this motor is a truncated cone structure, dubbed connector, which allows the 19.3 kb dsDNA genome to enter during maturation and to exit during infection[11,12] (Figure 1a). The phi29 motor (30 nm in dimension) constructed in 1987[13] is one of the strongest biomotors[14] assembled in vitro. The ability to produce such a motor outside its natural environment will have great potential to impact biology, engineering, medicine, and various other nanotechnological fields. Although the individual building blocks of the connector of different viruses share little sequence homology and exhibit large variations in molecular weight,[12,15−20] the connector complexes possess a significant amount of morphological similarity.[21] In the case of bacteriophage phi29, the structure of the connector has been determined to atomic resolution.[12,15] The connector ring consists of 12 subunits, with a central channel formed by three long α-helices of each subunit. The ring is 13.8 nm at its wide end and 6.6 nm at its narrow end. The internal channel is 6.0 nm at the wider end and 3.6 nm at the narrower end (Figure 1b). The wider end of the connector is located within the capsid, while the narrower end partially protrudes out of the capsid.

The novelty and ingenious design of such machines have inspired the development of biomimetics. In vitro, the biomimetic motor can be integrated into synthetic nanodevices.[22,23] In vivo, the artificial nanomotors can be used to load drugs, deliver DNA/RNA, pump ions, transport cargoes, or drive the motion of components in the heart, eye, or other sensing organs in the body.

We have previously reengineered the connector protein and inserted the connector into lipid bilayers.[24,25] The translocations of ions and dsDNA through the channel have been characterized to demonstrate the power of the phi29 connector for use in single DNA sensing and fingerprinting. In this study, we report that the phi29 motor channel exercises a one-way DNA traffic mechanism, and by using single channel conductance assays, we have identified the orientation of the channel in the lipid membrane and the direction of DNA trafficking to be from the N-terminal narrower end toward the C-terminal wider end.

In recent years, some reengineered protein channels[26−28] and chemically modified synthetic pores[29−31] have been reported to have ion rectifying capabilities by allowing ions to flow in one direction. For example, a mutant 7R- α-hemolysin has been shown to only allow ion transport under positive voltages, even at high ion concentrations.[26] By a different mechanism, chemically modified synthetic pores can be made to exhibit electronic diode-like properties.[32,33] However, native wild type protein channels have not been

* Address correspondence to: Peixuan Guo Vontz Center for Molecular Studies, ML#0508, 3125 Eden Avenue, Room 2308, University of Cincinnati Cincinnati, OH 45267. Phone: (513)558-0041. Fax: (513)558-0024. E-mail: guop@purdue.edu, guopn@ucmail.uc.edu.

† Both authors contributed equally to this work.

Received for review: 06/1/2010
Published on Web: 08/19/2010

DOI: 10.1021/nl101939e | *Nano Lett.* **2010,** *10,* 3620–3627

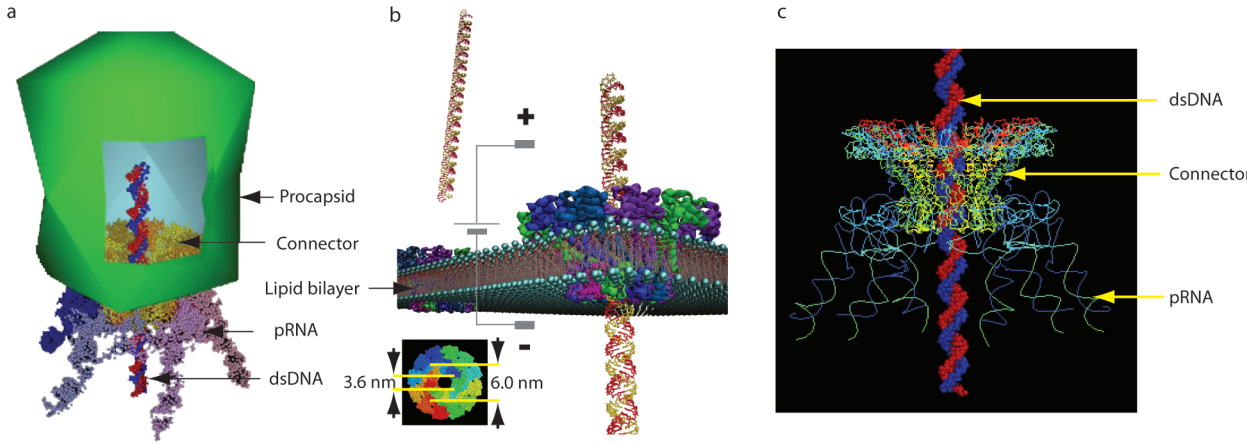

FIGURE 1. An illustration of DNA translocation through (a) a phi29 DNA packaging motor in vivo and (b) a membrane-embedded connector channel in vitro. (c) Three-dimensional structure of phi29 connector/dsDNA complex showing the counterchirality between the left-handed connector channel wall and the right-handed dsDNA.

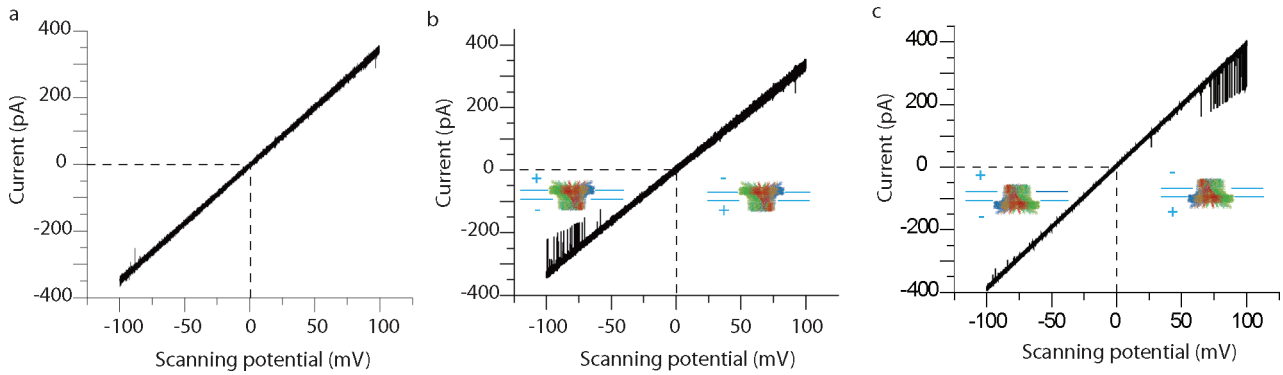

FIGURE 2. One-way traffic in DNA translocation through a single connector channel in a lipid bilayer under a ramping potential: (a) without DNA; (b, c) DNA added in both chambers with a single connector. The voltage is from −100 mV to +100 mV (2.2 mV/s).

reported to have rectifying behavior with regard to DNA translocation.

Results. ***The robust connector channel exhibited a two-way traffic property for ions with equal conductance under both positive and negative trans-membrane potentials.*** The purified connector was inserted into a planar lipid bilayer membrane (BLM) and thereby formed an artificial membrane channel.[24,25] Insertion of the connectors into the membrane was observed directly by the discrete stepwise increase of the current. Such observation enabled the direct counting of the number of channels inserted into each membrane. The step size of each current augment, representing the insertion of additional connector channels, was nearly identical for each channel. The conductance was uniform and did not display voltage gating properties under the conditions described in this report. In addition, the channel demonstrated a perfectly linear relationship with respect to the applied voltage and exhibited equal competencies in ion translocation in both directions under a positive and negative trans-membrane potential.[24,25]

One-way traffic of dsDNA was probed by applying a ramping potential to a membrane with a single channel. Given that the connector channel is inserted into the BLM via the fusion of the liposome/connector complex with the BLM, the orientation of the connector channel is random. It can be in a conformation with either the C-terminus facing the cis-chamber (the upper chamber with a ground electrode, where the liposome/connector complexes were added before insertion) or the N-terminus oriented toward the cis-chamber.

The application of a ramping potential to the BLM containing a single connector channel revealed a unidirectional translocation of dsDNA. A ramping voltage (2.2 mV s^{-1}) from −100 to +100 mV was applied to obtain the $I-V$ curves (Figure 2). The current−voltage relationship is perfectly linear, demonstrating well-behaved, uniform conductance of the channel. Due to the negative charge of the phosphate backbone, DNA generally migrates from the negative to the positive potential. Figure 2a shows a control experiment in the absence of dsDNA. When dsDNA was premixed in both the cis and trans chambers at identical concentration, DNA translocation can only be observed in one direction (Figure 2b,c). For each trial, DNA translocation occurred under either positive (Figure 2c) or negative trans-membrane potential (Figure 2b), depending on the orientation of the connector inserted in the BLM (the orientation was verified by a method using Nanogold described in a later section). The results

DOI: 10.1021/nl101939e | *Nano Lett.* **2010,** *10,* 3620–3627

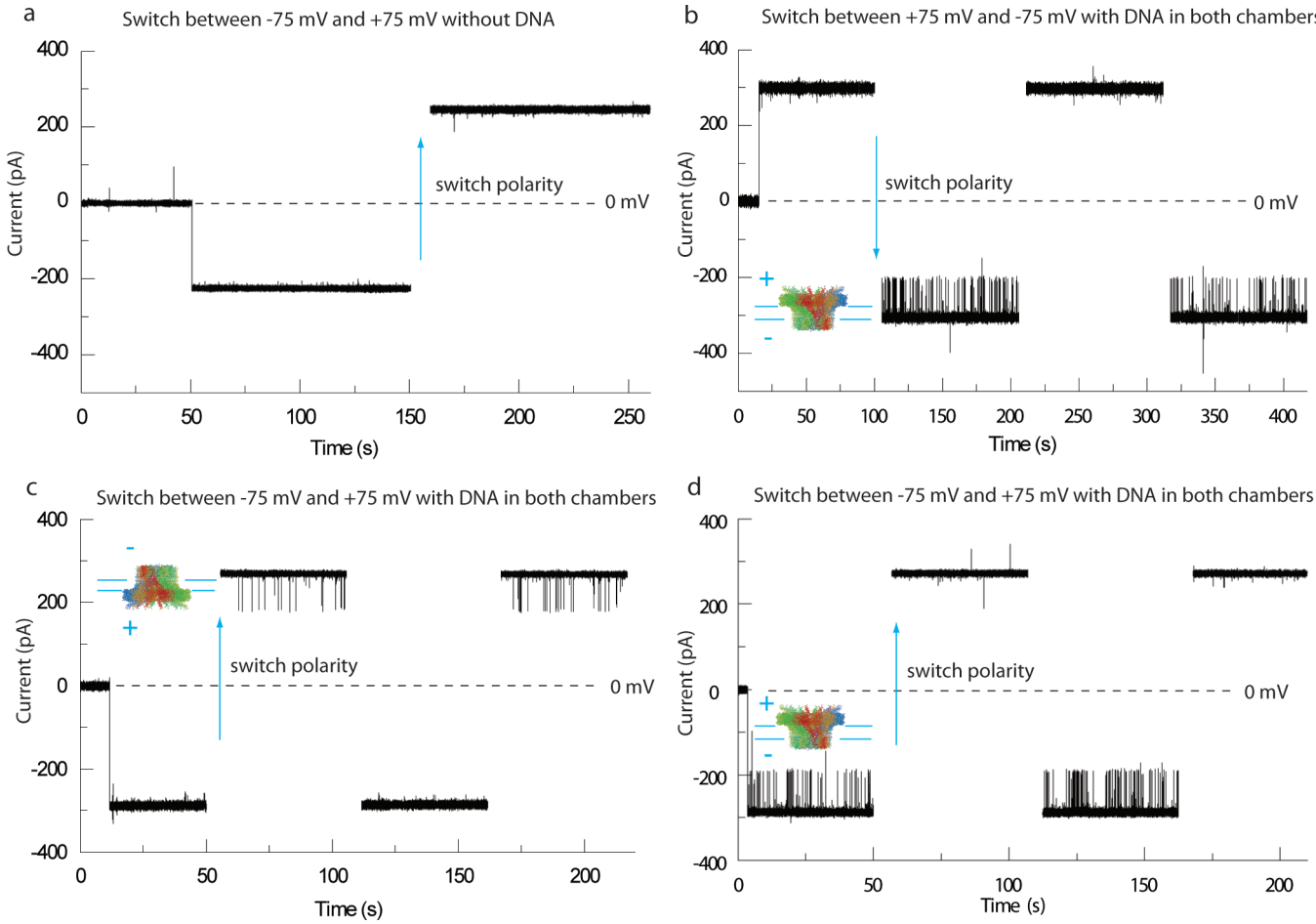

FIGURE 3. One-way traffic in DNA translocation through a connector channel in bilayers verified by switching polarity. (a) No DNA in either chamber; (b−d) The presence of DNA in both chambers where a single connector was inserted.

strongly support that when the connector is inserted in artificial lipid membranes, dsDNA can only pass through the connector channel in one direction. The same results were obtained with dsDNA of varying lengths (from 12 to 5500 bp) as well as for ssDNA (data not shown).

One-way traffic of dsDNA was probed by applying a constant holding potential and by switching the voltage polarity to a membrane with a single channel. Switching of voltage polarity revealed that the connector channel allowed only a unidirectional translocation of dsDNA. DNA was premixed in both chambers under a constant voltage. DsDNA translocation via the single-channel BLM could be turned on and off depending on the polarity of the voltage (Figure 3b−d). The correspondence to voltage switching was dependent upon the orientation of the connector in the BLM (the orientation was verified by a method using Nanogold described in a later section). For example, when there was no DNA translocation under positive potential, switching the voltage to negative potential resulted in dsDNA translocation (Figure 3b). Conversely, when there was no DNA translocation under negative potential, switching the voltage to positive potential resulted in dsDNA translocation (Figure 3c). Similarly, when dsDNA translocation was observed under negative potential, switching the voltage to positive potential resulted in no dsDNA translocation (Figure 3d). The results strongly support that when the connector is inserted in artificial lipid membranes, DNA can only pass through the connector channel in one direction. The same results were also confirmed under different voltages (data not shown).

One-way traffic of dsDNA was probed by quantification of DNA translocation frequency in the presence of multiple channels. If dsDNA only traverses through connector channels from one direction, the DNA translocation frequency would be affected by a different arrangement of connector orientation when multiple channels were inserted into the bilayer, regardless of the DNA concentration. The experiments in Figure 4 were carried out under a constant holding potential of −75 mV and in the presence of varying concentrations of dsDNA. The current traces with multiple connector insertions reflect the change in the frequency of DNA translocation events (represented in the histograms in Figure 4). When one additional connector was inserted with an appropriate orientation to allow DNA to pass, the frequency of DNA translocation increased (Figure 4a,b,d). When one additional connector was inserted with an opposite orientation that did not allow DNA to pass, the frequency of DNA

DOI: 10.1021/nl101939e | *Nano Lett.* **2010,** *10,* 3620–3627

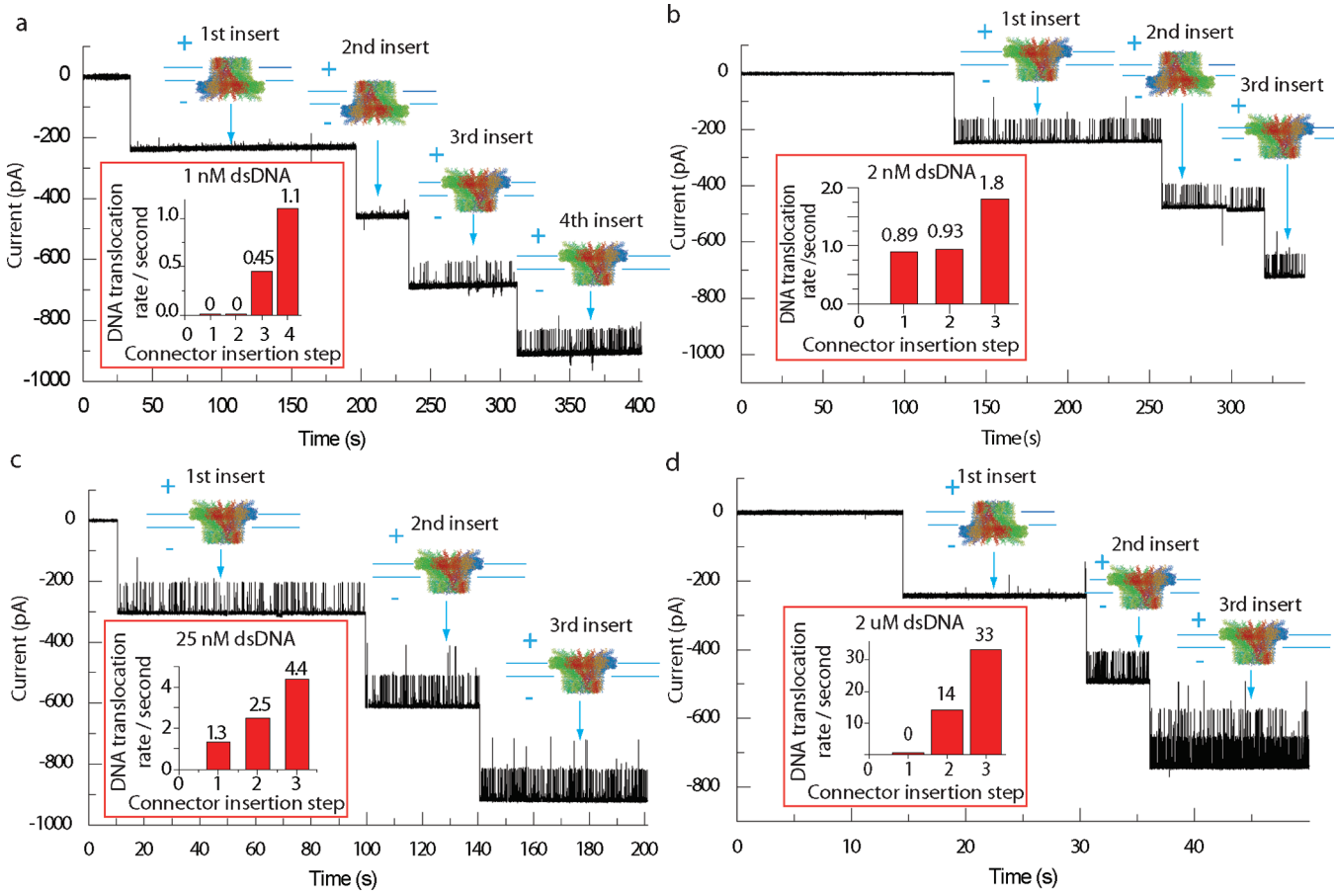

FIGURE 4. One-way traffic in DNA translocation through a connector channel reflected in the change of DNA translocation frequency related to the orientation of connectors in bilayers with multiple connector insertions. Various concentrations of DNA were premixed in both chambers before applying the voltage. Inset: For the individual experiments (a−d), the DNA translocation frequency after the insertion of each connector channel in the BLM is shown.

translocation did not change (Figure 4b). In either case, the frequency of DNA translocation did not decrease when additional connectors were inserted in the BLM.

The orientation of the connector was probed using Ni-NTA Nanogold targeted at C-terminal His-tag. To elucidate the orientation of the connector in the BLM, we used connectors with a His-tag incorporated into the wide-end C-terminus of each connector subunit gp10. The insertion of the terminal His-tag did not affect the folding or DNA packaging activity of the connector channel.[24] The experiments in Figure 5 were carried out under asymmetric ionic conditions.[34] (Also see Supporting Information.) A 1.8 nm Ni-NTA nanogold particle (150 pM) was used to bind to the His-tag at the C-terminus. The nanogold was premixed with the conductance buffer at only one side of the chamber. For example, if the nanogold is present in the trans side under single or multiple connector channel insertion conditions (Figure 5), it will only bind to the connector with its His-tagged C-terminal end oriented toward the trans chamber (Figure 5c) and will not bind to connectors with the N-terminus facing the trans side (Figure 5a). It was found that clear discrete stepwise blockage of the channel and a corresponding decrease in conduction appeared when a single connector with appropriate orientation for nanogold binding was present (Figure 5d). Binding of each nanogold particle resulted in 30% blockage in channel current (Figure 5d.). Such observations enabled the direct counting of the number of nanogold particles bound to each connector. The step size of each current reduction, resulting from the binding of one nanogold particle, was nearly identical, even in the case of membranes with multiple channels (data not shown).

The same concentration of dsDNA was added in both sides of the chamber to aid the appraisal of the DNA translocation direction, since dsDNA only migrates from the negative toward the positive potential due to its negatively charged phosphate backbone. On the basis of the placement of the nanogold in either the cis- or trans- side of the chamber (experimental design shown in Figure 5a,c,e) under a constant negative trans-membrane potential, the orientation of the connector embedded in the membrane could be determined. It was found that dsDNA translocated one way from the N-terminal narrow end toward the C-terminal wide end. For example, when nanogold was placed in the bottom trans chamber, nanogold binding was not observed while dsDNA translocation occurred, indicating that in this case,

DOI: 10.1021/nl101939e | *Nano Lett.* **2010,** *10,* 3620–3627

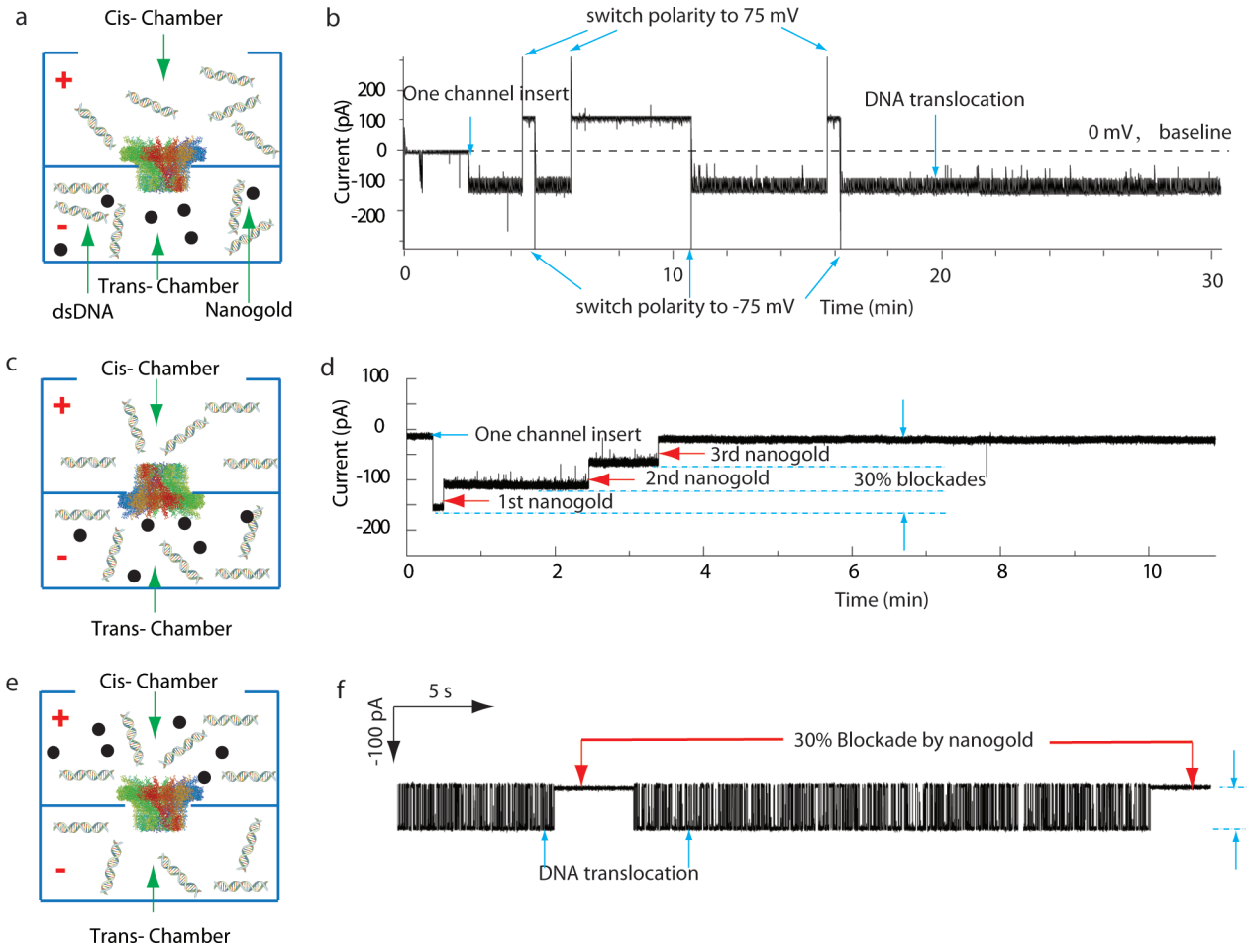

FIGURE 5. Probing the orientation of the connector using Ni-NTA Nanogold targeted at C-terminal His-tag. (a, c, and e) Illustration of strategy for orientation probing with equal concentration of dsDNA added to both cis and trans chamber and same amount of Ni-NTA Nangold for each experiment. (b) A 30 min current trace showing the translocation of dsDNA without blocking by Ni-NTA Nanogold added to the trans chamber. (d) A current trace showing three binding steps of Ni-NTA Nangold to C-His connector after addition of Ni-NTA to the bottom trans chamber. (f) A current trace showing the translocation of dsDNA and blocking of DNA translocation by Ni-NTA Nanogold added to the top cis chamber. For all these experiments, a trans-membrane potential of −75 mV was applied.

the C-terminus containing the His-tag was facing the upper cis chamber and the dsDNA translocated from the N-terminus at the bottom trans chamber that was negative (Figure 5b). Under the same conditions, in the other case where the connector is oriented such that the C-terminus is facing the trans chamber, stepwise binding of nanogold was observed without any DNA translocation (Figure 5d). In another scenario, when the nanogold was added to the upper cis chamber, dsDNA translocation occurred initially and was subsequently blocked, indicating that in this case the His-tagged C-terminus was facing the upper cis chamber, where nanogold binding occurs, and dsDNA translocated from the N-terminus facing the bottom trans chamber (Figure 5f).

Partially packaged dsDNA in the active motor remained within the channel without exerting a pushing force. The membrane-embedded connector with dsDNA translocation capacity provides a new system to study the mechanism of viral DNA packaging with an unconventional perspective. However, the mechanism of passive transport via electrical potential in the lipid membrane system might not be identical to the active packaging via ATP-driven motion force. Determination of the one-way traffic phenomenon in the active motor is very challenging. Varieties of experiments were carried out to explore whether the active motor incorporated in the procapsid also exhibits a one-way traffic mechanism, and the following findings were observed.

During the dsDNA translocation process, the active motor was turned off by adding a nonhydrolyzable ATP analogue, γ-S-ATP.[35] Both the completely and partially packaged dsDNA remained in the procapsid and did not show a reverse exit in the gradient under all centrifugation force tests (e.g., 149000*g*).[35,36] The finding agrees with the phenomena observed previously that dsDNA did not eject from the channel and remained within the channel of the DNA-packaging intermediates.[2,14,35] DNA packaging by the motor is an entropically unfavorable process and chemical energy from ATP hydrolysis is required for DNA translocation.[2,10]

DOI: 10.1021/nl101939e | *Nano Lett.* **2010,** *10,* 3620–3627

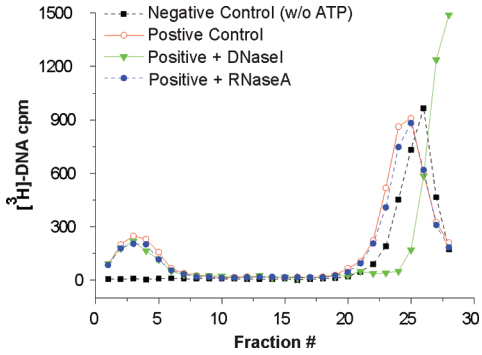

FIGURE 6. Sedimentation assays for DNA packaging and retention within the procapsid with [3H]-phi29 DNA via 5−20% sucrose gradient. DNA was packaged into the procapsid through the channel of phi29 DNA packaging motor with the in vitro phi29 DNA packaging system[67,68]). After DNA packaging, the samples were divided and digested with either DNase I or RNase A, respectively. All samples were loaded onto the top of the gradient and sedimented from right to left by ultracentrifugation followed by scintillation counting.

The pressure within viral procapsids gradually increases when longer and longer dsDNA are packaged as the space within the cavity of the procapsid becomes smaller and smaller.[2,14,35,37]

To argue for the one-way traffic property of phi29 DNA-packaging channel in an active motor and to rule out the possibility that dsDNA remaining inside the channel is due to the contributions of pRNA, gp16, and/or γ-S-ATP, sedimentation assays were performed. The fully packaged DNA and the DNA packaging intermediates were treated individually and in combination with DNase I and/or RNase A (Figure 6). The goal of DNase treatment is to exclude the possibility of any contact of motor components that could restrain the dsDNA from exiting. RNase A digestion will specifically exclude the possibility of pRNA and gp16 from contacting and holding the DNA. Since pRNA serves as a bridge between the motor and gp16,[38] RNase digestion will eliminate the fulcrum to prevent the exercise of force, if any, from pRNA and gp16 to dsDNA. Our data revealed that, when the DNA-packaging intermediates, with partial dsDNA within the channel and partial dsDNA outside the channel, were treated with DNase I or RNase A, or both, the partially packaged dsDNA stayed inside the procapsid and did not show a reverse exit in the gradient under highest centrifugation force (Figure 6). The data strongly support the conclusion that the motor channel in a living virion also exercises the one-way traffic property.

Discussion. During the last several decades of studies on viral DNA packaging motors, many models have been proposed to interpret the mechanism of motor action. These include (1) gyrase-driven torsion and relaxation;[39] (2) osmotic pump;[40] (3) ratchet mechanism;[41] (4) Brownian motion;[42] (5) 5-fold/6-fold mismatch connector rotating thread;[43] (6) supercoiled DNA wrapping;[44] (7) sequential action of motor components;[45] (8) electrodipole within central channel;[12] (9) connector contraction hypothesis.[46] All these models are very intriguing, but none has been supported by conclusive experimental data. A report that fusion of the connector protein with other accessory proteins either inside or outside the capsid did not affect phage T4 DNA packaging challenges the validity of any model involving portal rotation.[47] The 5-fold/6-fold mismatch connector rotating thread model[43] has been popular for more than 30 years, since this model might bring about a new mechanical motor prototype. Even within the last several years, several laboratories have persevered with intention to make up or search for a 5-fold ring to adapt their finding to this fascinating model. Unfortunately, recent studies in many viral DNA packaging motors reveal that the stoichiometry of motor components is not odd numbers, but even numbers.[48−51] The finding of an even number structure is consistent with the mechanism of many other well-studied DNA tracking motors[52−58]

Recently, Guo and Lee proposed a pushing or injection model.[59] In this model, the connector remains static; DNA translocation is induced by a DNA packaging enzyme or terminase, which pushes a certain length of DNA into the procapsid and then shifts to bind to a far distal region of the DNA and inserts an additional section. This model does not exclude the *socket wrench* rotating motion by the enzyme. The studies reported here provide direct evidence to prove the model.[59]

It is very interesting to observe the counterchirality between the left-handed phi29 connector channel and the right-handed dsDNA. The phi29 connector channel is composed of 12 copies of the protein gp10 with each existing as three-helices to encircle the channel, and exhibiting a left-handed configuration (Figure 1c). However, the regular viral dsDNA genome is the normal B-form DNA exhibiting a right-handed configuration. As far as the energy is concerned, it is expected that such an opposite configuration would favor the ejection of the dsDNA during infection and would not favor the packaging during assembly. However, our findings revealed a contrasting phenomenon: under an external electrical force, the channel favored DNA entry but blocked DNA exit, suggesting a very intriguing structure and motion mechanism for the motor. In this situation, the channel wall and the dsDNA constitute two counterparallel helices. It is possible that the sequential attraction between the negative charge of the phosphate backbone and the positive charge of the channel wall, which contains two 12-lysine rings (aa #200, 209) separated by 2 nm (and possibly two more rings at locations K234, K235),[12] will produce a stepwise propelling force for DNA translocation. It has been reported that the conformation of the phi29 connector is substantially changed after DNA packaging.[60,61] Such significant rearrangements of the connector after DNA packaging, a similar feature reported in other phage systems as well,[62−64] might change the channel configuration to reversely favor the DNA exit during infection.

The one-way traffic property is also evidenced in our previous publication (Figure 3g in ref 24), although the

DOI: 10.1021/nl101939e | *Nano Lett.* **2010,** *10,* 3620–3627

phenomenon was not realized at that point. Herein, our results obtained from both membrane-embedded connector channels and in vitro DNA packaging assays imply that during the packaging of dsDNA via the active motor, dsDNA travels in only one direction from the narrower end (N-) toward to the wider end (C-terminal) of the channel. Thus, the results suggest that dsDNA packaging is through an active pushing[65,66] by the motor ATPase gp16 in combination with a valve mechanism of the channel.[41]

Acknowledgment. We thank Feng Xiao and Ying Cai for constructing the recombinant connectors and Anne Vonderheide and Jia Geng for assistance in manuscript preparation. The research was supported by GM059944, and NIH Nanomedicine Development Center: Phi29 DNA Packaging Motor for Nanomedicine, through the NIH Roadmap for Medical Research (PN2 EY 018230). P.G. is a cofounder of Kylin Therapeutics, Inc.

Supporting Information Available. Description of the methods. This material is available free of charge via the Internet at http://pubs.acs.org.

REFERENCES AND NOTES

(1) Earnshaw, W. C.; Casjens, S. R. DNA packaging by the double-stranded DNA bacteriophages. *Cell* **1980**, *21*, 319–331.
(2) Guo, P.; Peterson, C.; Anderson, D. Prohead and DNA-gp3-dependent ATPase activity of the DNA packaging protein gp16 of bacteriophage ϕ29. *J. Mol. Biol.* **1987**, *197*, 229–236.
(3) Chemla, Y. R.; Aathavan, K.; Michaelis, J.; Grimes, S.; Jardine, P. J.; Anderson, D. L.; Bustamante, C. Mechanism of force generation of a viral DNA packaging motor. *Cell* **2005**, *122*, 683–692.
(4) Hwang, Y.; Catalano, C. E.; Feiss, M. Kinetic and mutational dissection of the two ATPase activities of terminase, the DNA packaging enzyme of bacteriophage lambda. *Biochemistry* **1996**, *35*, 2796–2803.
(5) Sabanayagam, C. R.; Oram, M.; Lakowicz, J. R.; Black, L. W. Viral DNA packaging studied by fluorescence correlation spectroscopy. *Biophys. J.* **2007**, *93* (4), L17–L19.
(6) Sun, S. Y.; Kondabagil, K.; Gentz, P. M.; Rossmann, M. G.; Rao, V. B. The structure of the ATPase that powers DNA packaging into bacteriophage t4 procapsids. *Mol. Cell* **2007**, *25*, 943–949.
(7) Guo, P.; Erickson, S.; Anderson, D. A small viral RNA is required for *in vitro* packaging of bacteriophage phi29 DNA. *Science* **1987**, *236*, 690–694.
(8) Guo, P.; Zhang, C.; Chen, C.; Trottier, M.; Garver, K. Inter-RNA interaction of phage phi29 pRNA to form a hexameric complex for viral DNA transportation. *Mol. Cell* **1998**, *2*, 149–155.
(9) Zhang, F.; Lemieux, S.; Wu, X.; St.-Arnaud, S.; McMurray, C. T.; Major, F.; Anderson, D. Function of hexameric RNA in packaging of bacteriophage phi29 DNA in vitro. *Mol. Cell* **1998**, *2*, 141–147.
(10) Moffitt, J. R.; Chemla, Y. R.; Aathavan, K.; Grimes, S.; Jardine, P. J.; Anderson, D. L.; Bustamante, C. Intersubunit coordination in a homomeric ring ATPase. *Nature* **2009**, *457* (7228), 446–450.
(11) Simpson, A. A.; Leiman, P. G.; Tao, Y.; He, Y.; Badasso, M. O.; Jardine, P. J.; Anderson, D. L.; Rossman, M. G. Structure determination of the head-tail connector of bacteriophage phi29. *Acta Crystallogr.* **2001**, *D57*, 1260–1269.
(12) Guasch, A.; Pous, J.; Ibarra, B.; Gomis-Ruth, F. X.; Valpuesta, J. M.; Sousa, N.; Carrascosa, J. L.; Coll, M. Detailed architecture of a DNA translocating machine: the high- resolution structure of the bacteriophage phi29 connector particle. *J. Mol. Biol.* **2002**, *315* (4), 663–676.
(13) Guo, P.; Grimes, S.; Anderson, D. A defined system for *in vitro* packaging of DNA-gp3 of the *Bacillus subtilis* bacteriophage phi29. *Proc. Natl. Acad. Sci. U.S.A.* **1986**, *83*, 3505–3509.
(14) Smith, D. E.; Tans, S. J.; Smith, S. B.; Grimes, S.; Anderson, D. L.; Bustamante, C. The bacteriophage phi29 portal motor can package DNA against a large internal force. *Nature* **2001**, *413*, 748–752.
(15) Simpson, A. A.; Tao, Y.; Leiman, P. G.; Badasso, M. O.; He, Y.; Jardine, P. J.; Olson, N. H.; Morais, M. C.; Grimes, S.; Anderson, D. L.; Baker, T. S.; Rossmann, M. G. Structure of the bacteriophage phi29 DNA packaging motor. *Nature* **2000**, *408* (6813), 745–750.
(16) Valpuesta, J. M.; Fujisawa, H.; Marco, S.; Carazo, J. M.; Carrascosa, J. Three-dimensional structure of T3 connector purified from overexpressing bacteria. *J. Mol. Biol.* **1992**, *224*, 103–112.
(17) Rishovd, S.; Holzenburg, A.; Johansen, B. V.; Lindqvist, B. H. Bacteriophage P2 and P4 morphogenesis: structure and function of the connector. *Virology* **1998**, *245*, 11–17.
(18) Newcomb, W. W.; Juhas, R. M.; Thomsen, D. R.; Homa, F. L.; Burch, A. D.; Weller, S. K.; Brown, J. C. The UL6 Gene Product Forms the Portal for Entry of DNA into the Herpes Simplex Virus Capsid. *J. Virol.* **2001**, *75* (22), 10923–10932.
(19) Kochan, J.; Carrascosa, J. L.; Murialdo, H. Bacteriophage Lambda Preconnectors: Purification and Structure. *J. Mol. Biol.* **1984**, *174*, 433–447.
(20) Donate, L. E.; Herranz, L.; Secilla, J. P.; Carazo, J. M.; Fujisawa, H.; Carrascosa, J. L. Bacteriophage T3 connector: three-dimensional structure and comparison with other viral head-tail connecting regions. *J. Mol. Biol.* **1988**, *201*, 91–100.
(21) Bazinet, C.; King, J. The DNA translocation vertex of dsDNA bacteriophages. *Annu. Rev. Microbiol.* **1985**, *39*, 109–129.
(22) Hess, H.; Vogel, V. Molecular shuttles based on motor proteins: Active transport in synthetic environments. *J. Biotechnol.* **2001**, *82* (1), 67–85.
(23) Soong, R. K.; Bachand, G. D.; Neves, H. P.; Olkhovets, A. G.; Craighead, H. G.; Montemagno, C. D. Powering an inorganic nanodevice with a biomolecular motor. *Science* **2000**, *290* (5496), 1555–1558.
(24) Wendell, D.; Jing, P.; Geng, J.; Subramaniam, V.; Lee, T. J.; Montemagno, C.; Guo, P. Translocation of double-stranded DNA through membrane-adapted phi29 motor protein nanopores. *Nat. Nanotechnol.* **2009**, *4*, 765–772.
(25) Jing, P.; Haque, F.; Vonderheide, A.; Montemagno, C.; Guo, P. Robust Properties of Membrane-Embedded Connector Channel of Bacterial Virus Phi29 DNA Packaging Motor. *Mol. BioSyst.* **2010**, Epub ahead of print. DOI:, 10.1039/C003010D.
(26) Maglia, G.; Heron, A. J.; Hwang, W. L.; Holden, M. A.; Mikhailova, E.; Li, Q.; Cheley, S.; Bayley, H. Droplet networks with incorporated protein diodes show collective properties. *Nat. Nanotechnol.* **2009**, *4* (7), 437–440.
(27) Aguilella, V. M.; Alcaraz, A. Nanobiotechnology: A fluid approach to simple circuits. *Nat. Nanotechnol.* **2009**, *4* (7), 403–404.
(28) Miedema, H.; Vrouenraets, M.; Wierenga, J.; Meijberg, W.; Robillard, G.; Eisenberg, B. A biological porin engineered into a molecular, nanofluidic diode. *Nano Lett.* **2007**, *7* (9), 2886–2891.
(29) Ali, M.; Ramirez, P.; Mafe, S.; Neumann, R.; Ensinger, W. A pH-tunable nanofluidic diode with a broad range of rectifying properties. *ACS Nano* **2009**, *3* (3), 603–608.
(30) Gracheva, M. E.; Vidal, J.; Leburton, J. P. p-n Semiconductor membrane for electrically tunable ion current rectification and filtering. *Nano Lett.* **2007**, *7* (6), 1717–1722.
(31) Yan, R.; Liang, W.; Fan, R.; Yang, P. Nanofluidic diodes based on nanotube heterojunctions. *Nano Lett.* **2009**, *9* (11), 3820–3825.
(32) Karnik, R.; Duan, C.; Castelino, K.; Daiguji, H.; Majumdar, A. Rectification of ionic current in a nanofluidic diode. *Nano Lett.* **2007**, *7* (3), 547–551.
(33) Sparreboom, W.; van den, B. A.; Eijkel, J. C. Principles and applications of nanofluidic transport. *Nat. Nanotechnol.* **2009**, *4* (11), 713–720.
(34) Wanunu, M.; Morrison, W.; Rabin, Y.; Grosberg, A. Y.; Meller, A. Electrostatic focusing of unlabelled DNA into nanoscale pores using a salt gradient. *Nat. Nanotechnol.* **2010**, *5*, 160–165.
(35) Shu, D.; Guo, P. Only one pRNA hexamer but multiple copies of the DNA-packaging protein gp16 are needed for the motor to package bacterial virus phi29 genomic DNA. *Virology* **2003**, *309* (1), 108–113.

DOI: 10.1021/nl101939e | *Nano Lett.* **2010,** *10,* 3620–3627

(36) Guo, P.; Peterson, C.; Anderson, D. Initiation events in *in vitro* packaging of bacteriophage ϕ29 DNA-gp3. *J. Mol. Biol.* **1987**, *197*, 219–228.
(37) Tsay, J. M.; Sippy, J.; Feiss, M.; Smith, D. E. The Q motif of a viral packaging motor governs its force generation and communicates ATP recognition to DNA interaction. *Proc. Natl. Acad. Sci. U.S.A.* **2009**, *106* (34), 14355–14360.
(38) Lee, T. J.; Guo, P. Interaction of gp16 with pRNA and DNA for genome packaging by the motor of bacterial virus phi29. *J. Mol. Biol.* **2006**, *356*, 589–599.
(39) Black, L. W. *In vitro packaging of bacteriophage T4 DNA. Virology* **1981**, *113*, 336–344.
(40) Serwer, P. The source of energy for bacteriophage DNA packaging: an osmotic pump explains the data. *Biopolymers* **1988**, *27*, 165–169.
(41) Serwer, P. Models of bacteriophage DNA packaging motors. *J Struct. Biol* **2003**, *141* (3), 179–188.
(42) Astumian, R. D. Thermodynamics and kinetics of a Brownian motor. *Science* **1997**, *276*, 917–922.
(43) Hendrix, R. W. Symmetry mismatch and DNA packaging in large bacteriophages. *Proc. Natl. Acad. Sci. U.S.A.* **1978**, *75*, 4779–4783.
(44) Grimes, S.; Anderson, D. The bacteriophage phi29 packaging proteins supercoil the DNA ends. *J. Mol. Biol.* **1997**, *266*, 901–914.
(45) Chen, C.; Guo, P. Sequential action of six virus-encoded DNA-packaging RNAs during phage phi29 genomic DNA translocation. *J. Virol.* **1997**, *71* (5), 3864–3871.
(46) Morita, M.; Tasaka, M.; Fujisawa, H. Structural and functional domains of the large subunit of the bacteriophage T3 DNA packaging enzyme: importance of the C-terminal region in prohead binding. *J. Mol. Biol.* **1995**, *245*, 635–644.
(47) Baumann, R. G.; Mullaney, J.; Black, L. W. Portal fusion protein constraints on function in DNA packaging of bacteriophage T4. *Mol. Microbiol.* **2006**, *61*, 16–32.
(48) Zhao, H.; Finch, C. J.; Sequeira, R. D.; Johnson, B. A.; Johnson, J. E.; Casjens, S. R.; Tang, L. Crystal structure of the DNA-recognition component of the bacterial virus Sf6 genome-packaging machine. *Proc. Natl. Acad. Sci. U.S.A.* **2010**, *107* (5), 1971–1976.
(49) Maluf, N. K.; Gaussier, H.; Bogner, E.; Feiss, M.; Catalano, C. E. Assembly of Bacteriophage Lambda Terminase into a Viral DNA Maturation and Packaging Machine. *Biochemistry.* **2006**, *45*, 15259–15268.
(50) Shu, D.; Zhang, H.; Jin, J.; Guo, P. Counting of six pRNAs of phi29 DNA-packaging motor with customized single molecule dual-view system. *EMBO J.* **2007**, *26*, 527–537.
(51) Xiao, F.; Zhang, H.; Guo, P. Novel mechanism of hexamer ring assembly in protein/RNA interactions revealed by single molecule imaging. *Nucleic Acids Res.* **2008**, *36* (20), 6620–6632.
(52) Lowe, J.; Ellonen, A.; Allen, M. D.; Atkinson, C.; Sherratt, D. J.; Grainge, I. Molecular mechanism of sequence-directed DNA loading and translocation by FtsK. *Mol. Cell* **2008**, *31* (4), 498–509.
(53) Skordalakes, E.; Berger, J. M. Structural insights into RNA-dependent ring closure and ATPase activation by the Rho termination factor. *Cell* **2006**, *127* (3), 553–564.
(54) Matias, P. M.; Gorynia, S.; Donner, P.; Carrondo, M. A. Crystal structure of the human AAA+ protein RuvBL1. *J. Biol. Chem.* **2006**, *281* (50), 38918–38929.
(55) McGeoch, A. T.; Trakselis, M. A.; Laskey, R. A.; Bell, S. D. Organization of the archaeal MCM complex on DNA and implications for the helicase mechanism. *Nat. Struct. Mol. Biol.* **2005**, *12* (9), 756–762.
(56) Hishida, T.; Han, Y. W.; Fujimoto, S.; Iwasaki, H.; Shinagawa, H. Direct evidence that a conserved arginine in RuvB AAA(+) ATPase acts as an allosteric effector for the ATPase activity of the adjacent subunit in a hexamer. *Proc. Natl. Acad. Sci. U.S.A.* **2004**, *101* (26), 9573–9577.
(57) Guo, S.; Tabor, S.; Richardson, C. C. The linker region between the helicase and primase domains of the bacteriophage T7 gene 4 protein is critical for hexamer formation. *J. Biol. Chem.* **1999**, *274* (42), 30303–30309.
(58) Mezard, C.; Davies, A. A.; Stasiak, A.; West, S. C. Biochemical properties of RuvBD113N: a mutation in helicase motif II of the RuvB hexamer affects DNA binding and ATPase activities. *J. Mol. Biol.* **1997**, *271* (5), 704–717.
(59) Guo, P. X.; Lee, T. J. Viral nanomotors for packaging of dsDNA and dsRNA. *Mol. Microbiol.* **2007**, *64*, 886–903.
(60) Tang, J. H.; Olson, N.; Jardine, P. J.; Girimes, S.; Anderson, D. L.; Baker, T. S. DNA poised for release in bacteriophage phi 29. *Structure* **2008**, *16* (6), 935–943.
(61) Tao, Y.; Olson, N. H.; Xu, W.; Anderson, D. L.; Rossmann, M. G.; Baker, T. S. Assembly of a Tailed Bacterial Virus and Its Genome Release Studied in Three Dimensions. *Cell* **1998**, *95*, 431–437.
(62) Kemp, P.; Gupta, M.; Molineux, I. J. Bacteriophage T7 DNA ejection into cells is initiated by an enzyme-like mechanism. *Mol. Microbiol.* **2004**, *53* (4), 1251–1265.
(63) Lebedev, A. A.; Krause, M. H.; Isidro, A. L.; Vagin, A. A.; Orlova, E. V.; Turner, J.; Dodson, E. J.; Tavares, P.; Antson, A. A. Structural framework for DNA translocation via the viral portal protein. *EMBO J.* **2007**, *26* (7), 1984–1994.
(64) Lhuillier, S.; Gallopin, M.; Gilquin, B.; Brasiles, S.; Lancelot, N.; Letellier, G.; Gilles, M.; Dethan, G.; Orlova, E. V.; Couprie, J.; Tavares, P.; Zinn-Justin, S. Structure of bacteriophage SPP1 head-to-tail connection reveals mechanism for viral DNA gating. *Proc. Natl. Acad. Sci. U.S.A.* **2009**, *106* (21), 8507–8512.
(65) Ray, K.; Sabanayagam, C. R.; Lakowicz, J. R.; Black, L. W. DNA crunching by a viral packaging motor: Compression of a procapsid-portal stalled Y-DNA substrate. *Virology* **2010**, *398* (2), 224–232.
(66) Ray, K.; Ma, J.; Oram, M.; Lakowicz, J. R.; Black, L. W. Single-molecule and FRET fluorescence correlation spectroscopy analyses of phage DNA packaging: colocalization of packaged phage T4 DNA ends within the capsid. *J. Mol. Biol.* **2010**, *395* (5), 1102–1113.
(67) Lee, C. S.; Guo, P. Sequential interactions of structural proteins in phage phi29 procapsid assembly. *J. Virol.* **1995**, *69*, 5024–5032.
(68) Lee, C. S.; Guo, P. In vitro assembly of infectious virions of ds-DNA phage ϕ29 from cloned gene products and synthetic nucleic acids. *J. Virol.* **1995**, *69*, 5018–5023.

DOI: 10.1021/nl101939e | *Nano Lett.* **2010,** *10,* 3620–3627